Effects of Bow Flare on Parametric Roll Characteristics of Surface Combatant

Woei-Min Lin, Kenneth M. Weems, and Sheguang Zhang
Advanced Systems and Technology Division
Science Applications International Corporation
4001 North Fairfax Dr., Suite 375, Arlington, Virginia, 22203, USA

Woei-min.lin@saic.com, Kenneth.m.weems@saic.com, and Sheguang.zhang@saic.com

ABSTRACT

The Large Amplitude Motions Program (LAMP) is used to study the bow flare effects on parametric roll of surface combatant. LAMP is a dynamic simulation program based on a potential flow solution of wave-body hydrodynamics. In the study, forward speed and metacentric height (GM) dependent viscous roll damping models, which are required to accurately predict the magnitude of parametric roll, were developed based on ship model roll decay tests. Numerical results showed the parametric roll for the tumblehome surface combatant, INSEAN Ship Model 2498, occurs at somewhat different speed range compared to the ship model test results. However, it was found that the occurrence of parametric roll depends strongly on parameters such as roll moment of inertia (Kxx), GM, wave frequency, ship speed, etc. LAMP was also used to study the effects of bow flare on parametric roll characteristics of ships. The three ONR top-side bodies – tumblehome (ONRTH), wall-sided (ONRWS), and flared (ONRFL) – were studied. The results are summarized in the paper.

1.0 INTRODUCTION

The phenomenon of parametric roll has drawn a great deal of attention in recent years as a result of significant cargo loss and damage sustained by a post-Panamax C11 class containership in late October 1998 [2]. Since this casualty, many research activities have been initiated to better understand the parametric roll phenomenon, classification societies have begun to develop guides for the assessment of parametric roll resonance in the design of container carriers [8], and several monitoring systems have been developed to assist ship operation in avoiding the occurrence of parametric roll during voyages.

Many of the studies of the parametric roll phenomenon have been based on hydrostatic approaches or potential flow solution of wave-body hydrodynamics. One of the key factors in predicting parametric roll accurately is roll damping. Using hydrostatics or potential flow based methods, viscous effects are not included and roll damping has to be added using external models. For example, in examining the parametric roll phenomenon of the C11 containership, roll damping models were built for the LAMP (Large Amplitude Motions Program) System using model-scale roll decay tests [2]. Viscous CFD (Computational Fluid Dynamics) methods, such us unsteady Reynolds Averaged Navier-Stokes (URANS), can also be used directly to provide a more complete solution of parametric roll phenomenon as recently demonstrated in [3].

One of the findings of the research work on parametric roll is the relationships between the nonlinear roll restoring related to ship bow flare and the likelihood of occurrence of parametric roll in different sea conditions. France, *et al.* [2] demonstrated different parametric roll behaviour for a standard Series 60 (C_B = 0.7) hull form with different topsides geometry. In a severe sea condition, the ship starts to show significant parametric roll only when the bow flare was increased to 40 degrees. With recent interest in novel hull form design for naval surface combatants, it is desirable to study the vulnerability of these designs to parametric roll, especially the influence of topside geometry on parametric roll characteristics.

In the effort described in this paper, LAMP was used to study the parametric roll phenomenon of a notional surface combatant with identical underwater and waterline geometry but different topside shapes. The three ONR topside shape variants: tumblehome (ONRTH), wall-side (ONRWS), and flared (ONRFL) were used in this study to understand the effect of bow flare on the parametric roll phenomenon. The roll damping models used in LAMP were derived using the ship model roll decay test results [3]. The LAMP predictions of parametric roll of the ONR tumblehome surface combatant were compared with model test results from [3].

In the current paper, Section 2 gives a general description of the LAMP ship dynamic simulation environment. Section 3 gives several examples of parametric roll and comparison with model test data. Section 4 discusses the effects of the bow flare on parametric roll characteristics.

2.0 THE LAMP (LARGE AMPLITUDE MOTIONS PROGRAM) SYSTEM

The LAMP System is a time-domain simulation model specifically developed for computing the motions and loads of a ship operating in extreme sea conditions. LAMP System development began with a 1988 DARPA (Defense Advanced Research Projects Agency) project for advanced nonlinear ship motion simulation, and has continued under the sponsorship of the U.S. Navy, U.S. Coast Guard, the American Bureau of Shipping (ABS), and Science Applications International Corporation's (SAIC) internal R&D program.

LAMP uses a time-stepping approach in which all forces and moments acting on the ship, including those due to the wave-body interaction, appendages, control systems, and green-water-on-deck, are computed at each time step and the 6-DOF equations of motions are integrated in the time-domain using a 4^{th}-order Runge-Kutta algorithm. In addition to motions, LAMP also computes main hull-girder loads using a rigid or elastic beam model and includes an interface for developing finite-element load data sets from the 3-D pressure distribution [8, 9].

The core of the LAMP System is the 3-D solution of the wave-body hydrodynamic interaction problem in the time-domain [4, 5]. A 3-D disturbance velocity potential is computed by solving an initial boundary value problem using a potential flow boundary element or "panel" method. A combined body boundary condition is imposed that incorporates the effects of forward speed, the ship motion (radiation), and the scattering of the incident wave (diffraction). The potential is computed using either a hybrid singularity model that uses both transient Green functions and Rankine sources [6], or a Rankine singularity model with a damping beach condition. Once the velocity potential is computed, Bernoulli's equation is then used to compute the hull pressure distribution including the second-order velocity terms.

The disturbance velocity potential can be solved either over the mean wetted surface (the "body linear" solution) or over the instantaneously wetted portion of the hull surface beneath the incident wave (the "body nonlinear" approach). In either case, it is assumed that both the radiation and diffraction waves are small compared to the incident wave and the incident wave slope is small so that the free-surface boundary conditions can be linearized with respect to the incident-wave surface. Similarly, the incident wave forcing (Froude-Krylov) and hydrostatic restoring force can also be computed either on the mean wetted surface or on the wetted hull up to the incident wave.

The combinations of the body linear and body nonlinear solutions of the perturbation potential and the hydrostatic/Froude-Krylov forces provide multiple solution "levels" for the ship-wave interaction problem. These levels are:

- LAMP-1 (Body linear solution): Both disturbance potential and hydrostatic/Froude-Krylov forces are solved over the mean wetted hull surface.
- LAMP-2 (Approximate body nonlinear solution): The disturbance potential is solved over the mean wetted hull surface while the hydrostatic/Froude-Krylov forces are solved over the instantaneous wetted hull surface.
- LAMP-3 (Approximate body nonlinear solution with large lateral displacements): similar to LAMP-2, but the hydrodynamic formulation is revised so that large lateral displacements and yaw angles are accounted for; this allows accurate maneuvering simulations.
- LAMP-4 (Body nonlinear solution): Both the perturbation potential and the hydrostatic/Froude-Krylov forces are solved over the instantaneous wetted hull surface.

Depending on the ship geometry and operating conditions, body-nonlinear hydrodynamics and nonlinear incident wave effects can be important. For most ship motion and wave load problems, the most practical level is the "approximate body-nonlinear solution" (LAMP-2), which combines the body-linear solution of the disturbance velocity potential with body-nonlinear hydrostatic-restoring and Froude-Krylov wave forces. This approach captures a significant portion of nonlinear effects in most ship-wave problems at a fraction of the computational effort for the general body-nonlinear formulation. This is the wave-body hydrodynamic approach used in most of the current parametric roll study.

In order to evaluate the statics-based approach toward dynamic stability analysis, a "hydrostatics-only" solution has been implemented which includes the body-nonlinear hydrostatics/Froude-Krylov forces but entirely neglects the wave-body hydrodynamic disturbance except for externally specified damping coefficients. This calculation, which has been designated LAMP-0, is intended to evaluate the effectiveness of simplified methods for determining the occurrence of parametric roll.

In order to have a complete dynamic simulation of a ship in waves, LAMP also includes a number of models for effects that are not included in the pressure distribution computed using the potential flow solution of the wave-body interaction but that still exert a force or moment that will impact the motion and/or loads on the ship. These "non-pressure" force models include effects such as viscous roll damping, propeller thrust, bilge keels, rudder and anti-rolling fins, mooring cables, internal tanks, and other systems. Because of the general time-domain approach, these non-pressure force models can include arbitrary nonlinear dependency on the motions, etc. For example, adjustable viscous roll damping models have been implemented with up to multiple order terms in the roll angle and velocity that allow the roll damping to be "tuned" to match experimental values by simulating roll decay tests.

Because these non-pressure force models run concurrently with the hydrodynamic calculation in the time domain, the models can include active or passive control systems that can be defined with the same types of physical inputs and outputs as the actual ship-board system. Standard built-in control models include a PID (proportional, integral, and derivative) course-keeping rudder control algorithm and a rudder servo model for maintaining proper ship-heading in oblique or short-crested seaway cases.

The LAMP code is structured so that new or modified time domain models of force actuators and/or control systems can be implemented into the motion and loads calculations in a fairly straightforward way. LAMP's ability to implement such models, coupled with its nonlinear physics-based solution of the wave-body hydrodynamics problem, makes it a very practical tool for general ship performance assessment.

3.0 EXAMPLES OF SHIP PARAMETRIC ROLL

Two ship parametric roll examples are discussed in this section. The first example is the C11-Class post-panamax containership [2]. The ship has large bow flare and long over-hang stern that have been found to be susceptible to parametric roll in heavy seas. The second example is a tumblehome ship, INSEAN Ship Model 2498, which experiences parametric roll in specific wave conditions when the roll natural period is about twice the encounter incident wave period. LAMP was used for parametric roll study for both cases. Comparisons with model test data are presented and discussed.

3.1 Parametric Roll of C11 Containership

In this section, a Post-Panamax C11-class containership is used as an example to illustrate the parametric roll phenomena the LAMP predictions of parametric roll. The body plan and a 3-D view of the geometry of the ship are shown in Figure 1. The ship length (Lpp) is 262 m, the beam is 40 m, and the design draft is 12.36 m. As can be seen in the figure, the ship has a very large bow flare and long over-hang stern. These are the typical features that can cause parametric roll in severe sea conditions.

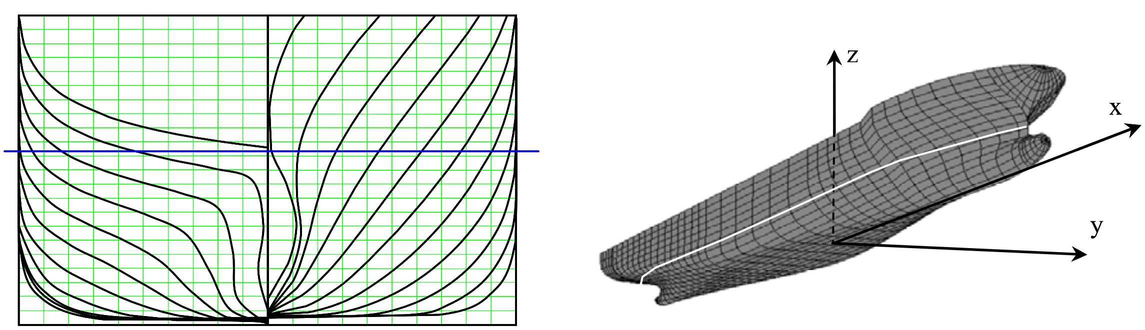

Figure 1: Lines (left) and 3-D geometry (right) of Post-Panamax C11 class containership

As described in [2], a series of LAMP simulations for the C11-Class containership were performed for comparison to MARIN model tests. These simulations to investigate parametric roll were performed at the same load condition utilized for the MARIN model tests.

In the simulation runs, the magnitude of the roll response during parametric excitation is dictated in large part by the amount of viscous damping in the roll degree of freedom. To account for these damping effects in LAMP, an empirical roll damping model was established from the roll decay model tests at various speeds. For the C11 investigation, the LAMP-2 roll decay response was tuned to match the experimental results by specifying an equation with up to cubic order terms of roll angle and roll velocity. To verify the tuned roll-damping model in the LAMP System, comparisons to both roll decay tests and regular wave parametric roll tests were performed. The comparisons of roll decay coefficients between the tuned LAMP-2 simulations and roll decay tests at 5, 10, and 15 knots are shown in Figure 2.

The roll and pitch motion comparison between the LAMP prediction with fixed forward speed and the full 6 degree-of-freedom experimental results in head regular waves are shown in the left-hand side of Figure 2. The results in right-hand side of Figure 2 illustrate the accuracy of LAMP-2 in predicting the head sea parametric roll phenomenon in regular waves.

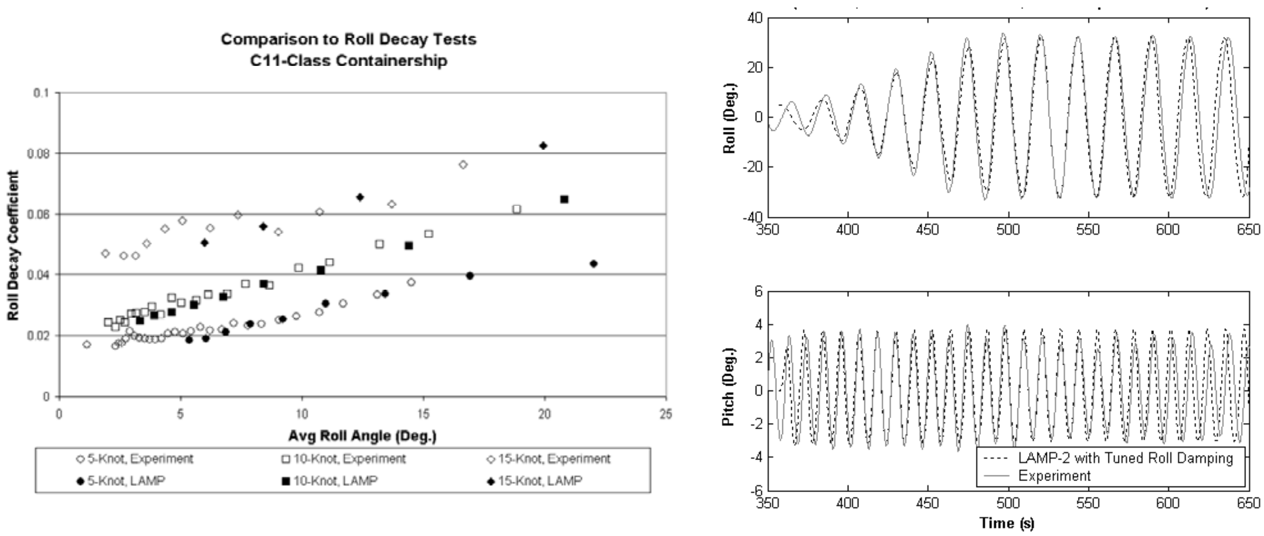

Figure 2: (Left) Tuning of roll damping for LAMP; (Right) regular waves comparison at 10 knots (Tw=14s, Hw=8.4m) (From [2])

3.2 Parametric Roll of a Tumblehome Ship

The second example is a tumblehome ship, INSEAN Ship Model 2498. This model is a geosim of the tumblehome variant of the ONR Topsides series of surface combatants (NSWCCD Model 5613, or ONRTH). A description of the INSEAN ship model 2498 is given in section 3.2.1. Using a similar procedure to the one used for the C11 containership, LAMP roll damping models were derived based on ship model test results. These numerical roll damping models and the process of determining these models are discussed in section 3.2.2. Sample results of the parametric roll behaviour for the INSEAN ship model 2498 at different speed and GM values are presented and discussed in section 3.2.3.

3.2.1 Description of INSEAN Ship Model 2498

The body plan and profile of INSEAN ship model 2498 are shown in Figure 3. The principal dimensions of the model are given in Table 1. The model tests were done at three different GM values. The roll moment of inertia values (Kxx) for the ship model are different for the different GM values. These differences were found to have a strong effect on the dynamic behaviour for the ship.

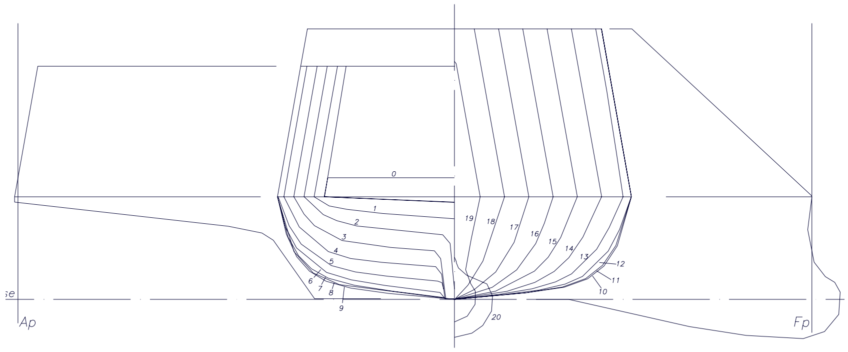

Figure 3: INSEAN Ship Model 2498 body plan and profile (from [7])

Table 1: Principal dimensions of the INSEAN ship model 2498 (From [7])

ONR Tumblehome Surface Combatant (Model Scale Ratio, λ = 46.6)		
	Original Specification	INSEAN Ship Model 2498
L_{PP}	3.305 m	3.305 m
Draft (T)	118 mm	118 ± 0.5 mm
Beam (B_{WL})	403 mm	Not verified.
Displ. (∇)	84.74 10^{-3} m^3	84.74 10^{-3} m^3
LCG	1708 mm (Aft of FP)	1708 ± 1 mm
KG	165 mm	165 ± 1 mm
GM	43 mm	A) 43 ± 1 mm B) 38 ± 1 mm C) 33 ± 1 mm
K_{XX}	0.153 m (38% B_{WL})	A) 0.123 m B) 0.125 m C) 0.127 m
$K_{YY} = K_{ZZ}$	0.826 m (25% L_{PP})	0.737 m (22% Lpp)

3.2.2 Viscous Roll Damping Models for INSEAN Ship Model 2498

Viscous roll damping is modelled in LAMP with several different empirical formulas which may include specified roll damping coefficients. In the study, a two-parameter roll damping model is used,

$$M_{Roll} = -\mu \bullet 2\sqrt{G_M Mg(I_{XX} + A_{XX})} \bullet V_{Roll} - \mu_2 \bullet \left|V_{Roll}\right| \bullet V_{Roll}$$

where GM is the transverse metacentric height; M is the ship mass; g is the gravity acceleration; I_{XX} and A_{XX} are the mass moment of inertia and added mass moment of inertia (infinite frequency) with respect to the longitudinal axis; V_{Roll} is the roll velocity; μ and μ_2 are linear and second order roll damping coefficients, respectively.

Since the parametric roll is directly related to the roll damping characteristics, determining the roll damping coefficients becomes an important task in setting up the potential-flow-based calculations. The procedure adopted is to first tune the damping coefficients based on INSEAN's experimental data [3] and to then interpolate/extrapolate coefficients for each combination of speed and GM values that is analyzed. Following the specifications of nine roll decay experiments, LAMP-2 runs are carried out for Froude number (Fn) = 0.05, 0.2 and 0.35 and GM = 33 mm, 38 mm and 43 mm. The initial roll angle is set to 30 degrees. The damping coefficients μ and μ_2 are adjusted to obtain the best match between the LAMP simulation and the experimental measurements. The tuned values are listed in Table 2, where μ is non-dimensional and μ_2 is in units of [kg*m^5].

Table 2: The roll damping coefficients tuned from the experimental data

	GM = 33 mm	GM = 38 mm	GM = 43 mm
Fn = 0.05	$\mu = 0.035$ $\mu_2 = 0.455$	$\mu = 0.01$ $\mu_2 = 0.455$	$\mu = 0.01$ $\mu_2 = 0.228$
Fn = 0.20	$\mu = 0.055$ $\mu_2 = 0.228$	$\mu = 0.02$ $\mu_2 = 0.319$	$\mu = 0.02$ $\mu_2 = 0.228$
Fn = 0.35	$\mu = 0.1$ $\mu_2 = 0.228$	$\mu = 0.05$ $\mu_2 = 0.228$	$\mu = 0.03$ $\mu_2 = 0.046$

Using these coefficients, the roll decay time histories for Fn = 0.2 with LAMP-2 are plotted in Figure 4 for GM = 33, 38 and 43 mm cases, respectively. In Figure 4, the peak of the experimental roll amplitudes are shown as black squares and the LAMP-2 results are red lines. The general trend is that for the given Fn, the roll decays faster with smaller GM than the larger GM. It shows that using the two-parameter roll damping model, LAMP-2 calculations generally match the experimental roll decay time histories, especially for the first four to five cycles. However, it is noticed that in the later stage of the roll decay for larger GMs (e.g. GM = 38 and 43 mm), the calculated roll period drifts from the experiment values. This appears to indicate that the two-parameter roll damping model may not have fully captured the roll damping characteristics of the tumblehome ship and further improvement for this model may be needed.

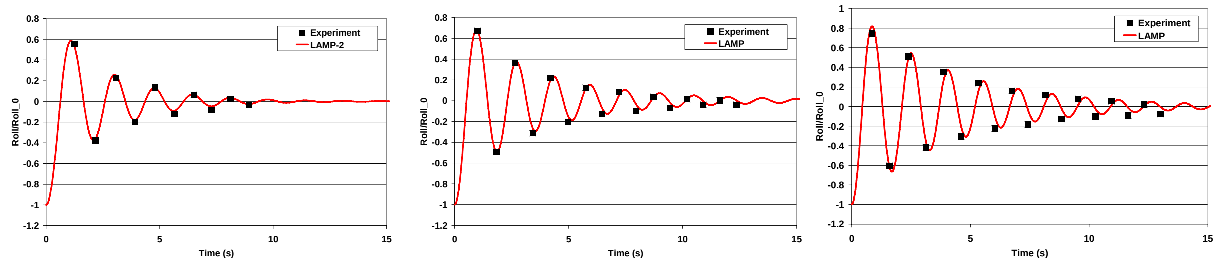

Figure 4: Roll decay time history comparisons between model test results and LAMP predictions (using tuned damping models) for Fn=0.2 and GM=33mm (left), GM=38mm (middle), and GM=43mm

To further explore the nonlinearity of roll motions of the tumblehome ship, the roll periods are estimated from each cycle of the experimental roll decay data and plotted versus roll amplitude in Figure 5. This plot clearly shows that the roll period varies dramatically as the roll amplitude changes. The increase in roll period with amplitude is primarily a result of the tumblehome top hull's reduced static restoring moment with heel. Since the parametric roll happens at roll period / pitch period ~ 2, this characteristic indicates that the incident wave period and amplitude has to be highly tuned for the tumblehome ship to have parametric roll. This characteristic also is very different from that of the C11 containership for which the natural roll period is fairly independent from the roll amplitude up to about 35 degrees.

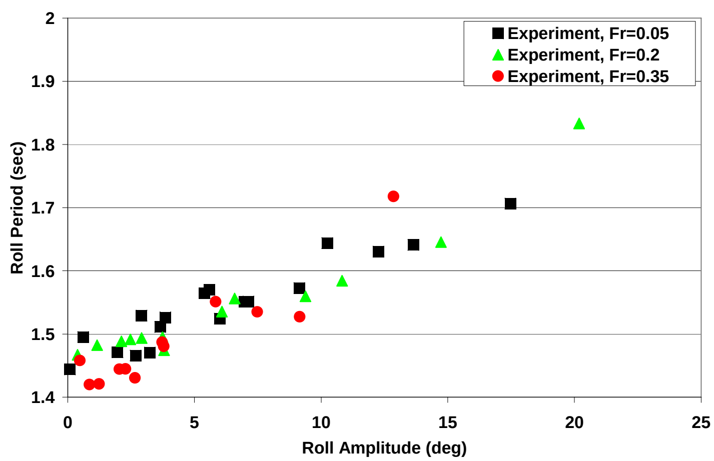

Figure 5: Roll period vs. roll amplitude for ONRTH, GM=38 mm based on INSEAN experiments

3.2.3 Sample Parametric Roll Results of INSEAN Ship Model 2498

Having demonstrated the roll motion characteristics in the previous section, this section gives some LAMP-2 results for parametric roll calculations using the INSEAN ship model 2498. The results are compared to the model test data and the differences are discussed. In the numerical setup, the simulation conditions are set to be as close to the experiment as possible, including input hull geometry, principal dimensions, ship speeds, degree of freedoms, incident waves, and initial conditions. Two sets of calculations are performed with the same settings as specified in the experiment, one with GM = 33 mm and the other with GM = 38 mm. Both use the same wave slope ka =2πa/λ= 0.115. No parametric roll was found for the GM = 43 mm configuration.

For the set of GMs and incident wave conditions, a series of LAMP-2 runs are performed to identify the occurrence of the parametric roll as a function of Froude number. The roll damping coefficients for each particular Fn is obtained from Table 2 through interpolation/extrapolation. The range of the occurrence of the parametric roll is illustrated in Figure 6, which plots the regular roll amplitude GM = 33 mm, a = 60 mm on the left and GM = 38 mm, a = 60 mm and a = 72 mm on the right. The experimental results are shown in black.

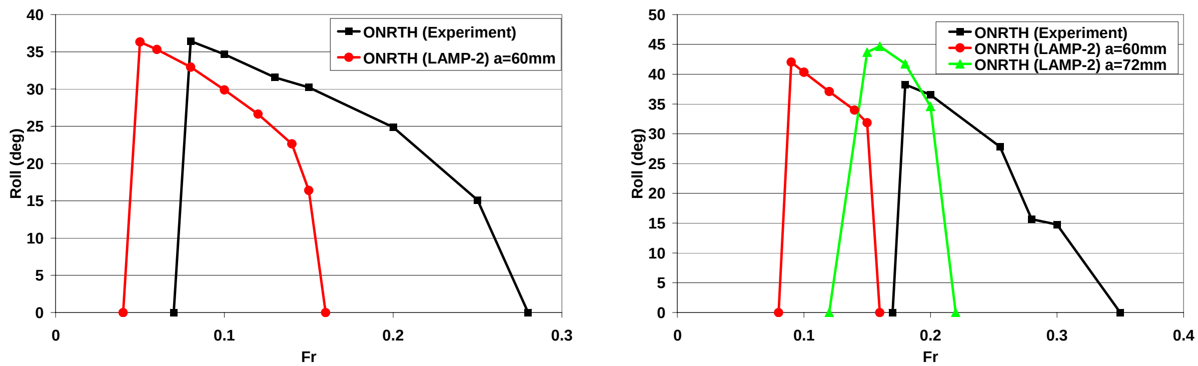

Figure 6: Roll amplitude *vs.* Froude number for ka=0.115, GM=33 mm (left) and GM=38 mm

For GM = 33 mm case, the range of the parametric roll in the LAMP-2 calculations is from Fn = 0.04 to 0.16 while the experiment is from Fn = 0.07 to 0.28. This predicted range of parametric roll is shifted to a lower Fn and covers a narrower range than the experiment. The maximum roll amplitude of the parametric roll, however, is similar between the calculation and the experiment. For GM = 38 mm, a = 60 mm, the calculation and the experiment differ in both the range of Fn and the roll amplitude.

A number of numerical tests have been conducted to explore the cause of such differences. It has been found that the parametric roll for this particular ship model is very sensitive to ship speeds, incident wave frequency, amplitudes, phases, roll damping coefficients, initial conditions, Kxx, Kyy, and GM values. A slight change in any one of these quantities often results in very different results. An illustration of this characteristic is shown in Figure 7. The left-had side figure shows the comparison of the numerical results and the model test results for the case with GM = 38 mm, Fn = 0.2, a = 60 mm, and ka = 0.115. The experiment shows parametric roll, while with the exact same settings, LAMP-2 shows no parametric roll. In this figure, the experimental results are shifted to the left to make them coincide with the first cycle in roll in the numerical results. It is interesting to observe that initial roll frequency from the model test and that from LAMP-2 are very similar. But, when the roll starts to decay in LAMP-2 results, the predicted roll period becomes smaller.

The right-hand figure of Figure 7 shows the roll and pitch motion time history of predicted parametric roll of the same tumblehome ship. In this case, GM, Fn, and ka = 0.115 values are all the same as before, but the wave frequency was reduced by 8%. As a result, the wave amplitude was increased from 60 mm to 72 mm. The LAMP-2 calculation predicts speed-range of parametric roll is shown on the right in Figure 6. Because of this change in the wave condition, the zone of the parametric roll is shifted to the right towards that of the experiment.

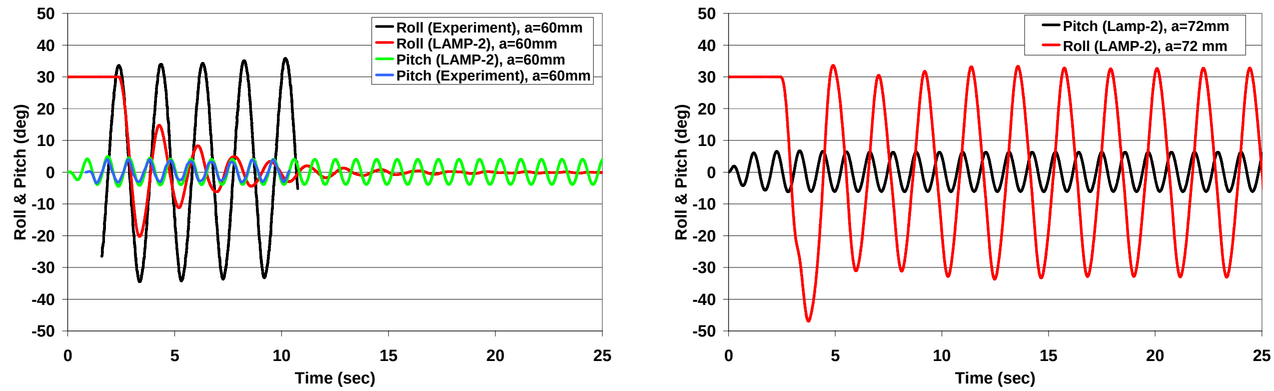

Figure 7: Roll and pitch time history comparisons for GM=38 mm, Fn=0.2, ka=0.115, a=60 mm (left) and a=72 mm (right)

Please note that the two curves on the right plot in Figure 7 are based on different wave lengths, i.e. the wave length is about 1 ship length in the experiment, while about 1.2 ship length in the calculation. This may indicates that: (1) the natural roll period in the calculation maybe longer than the experiment, which could be the case as shown in the later stage of the roll decay results in the middle figure in Figure 4 for GM = 38 mm and Fn = 0.2; (2) the two-parameter roll damping model may not be good enough to reflect the roll damping characteristics of the tumblehome ship, and (3) body-nonlinearities in hydrodynamics may be a factor to consider.

4.0 EFFECTS OF BOW FLARE ON PARAMETRIC ROLL

As noted earlier, one of the findings of the research work on parametric roll is the strong relationship between ship bow flare and the occurrence of parametric roll in different sea conditions. France, *et al.* [2] showed changes in parametric roll behaviour of a standard Series 60 (C_B = 0.7) hull form with changes in the topside geometry. In a severe sea condition, the ship starts to show significant parametric roll only when the bow flare was increased to 40 degrees. With recent interest in novel hull form design for naval surface combatants, it is desirable to study the vulnerability of these designs to parametric roll, especially the influence of topside geometry on parametric roll characteristics.

The three ONR Topside hull form variants were used in this study to investigate the effect of bow flare on the parametric roll phenomenon. The three hulls have the same geometry beneath the design waterline but have different topsides: wall-sided (ONRWS), flared (ONRFL), and tumblehome (ONRTH). These three models are shown in Figure 8. The principal particular of these three hulls are given in Table 1. Other than the top-side geometries themselves, the primary difference of the three models is the GM value that would be required by conventional stability criteria. The required minimum GM for ONRTH is 43 mm, the GM for ONRWS is 24 mm, and the GM for ONRFL is 4 mm. This difference shows how ship stability concerns require a higher GM for the tumblehome design because of the rapid reduction in the restoring moment at large heel angles. However, the tumblehome ship is typically less susceptible to parametric roll compared to ships with bow flare. In the current study, all three GM values are used for each ship to explore the GM effects on parametric roll.

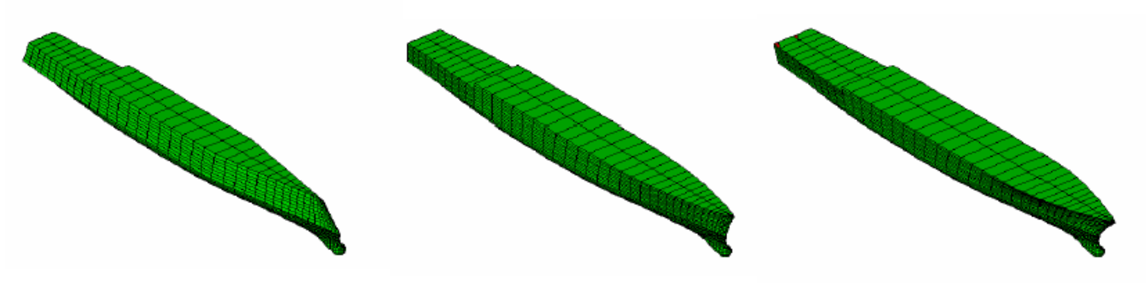

Figure 8: ONR top-side body, ONRTH (left), ONRWS (center), and ONRFL (right)

A systematic study of parametric roll for these three hulls in different wave conditions (wave slope ka = 0.115 and 0.156) was carried out using LAMP-2. In this study, no bilge keels were used. In addition, due to lack of a roll damping model test for ONRWS and ONRFL, the roll damping coefficients used for them are assumed to be the same as those for ONRTH, GM = 38 mm ship. Figure 9 shows the roll decay time history calculations for the three ONR topside hulls with the identical numerical setup except for topside geometries (Fn = 0.2, GM = 38 mm, $\mu = 0.02$, $\mu_2 = 0.319$, etc.). This figure shows that the topside geometry has a significant influence on the roll period at larger roll angles; with ONRFL having shortest roll period and ONRTH the longest. These characteristics will be reflected in the parametric roll behaviour.

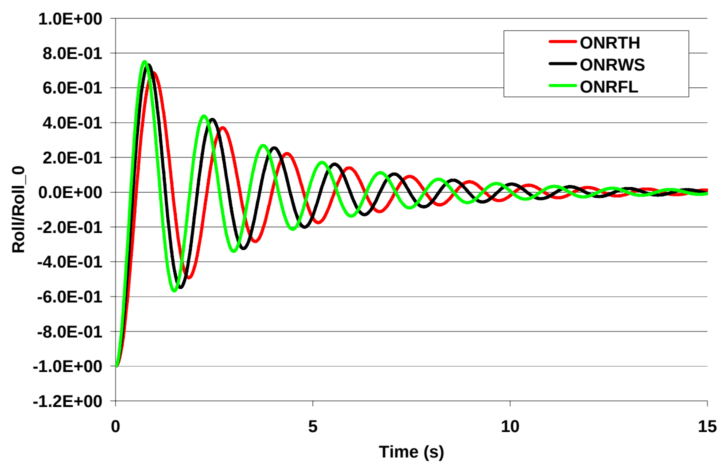

Figure 9: Roll decay time histories for ONRTH, ONRWS and ONRFL; GM=38 mm, Fr=0.2

The results of the simulations in waves are summarized below.

- For GM = 33 and 38 mm with the same running conditions as those in Figure 6 for ONRTH – parametric roll is not seen for either ONRFL and ONRWS.
- For GM = 24 mm (the criteria GM for ONRWS) with ka = 0.115 and 0.156 – parametric roll is seen for ONRWS.

- For GM = 4 mm (design GM for ONRFL) with ka=0.115 – parametric roll is not seen for ONRFL.
- Using GM=24 mm for ONRFL with ka=0.115 and 0.156 – parametric roll is seen for ONRFL.
- Using GM=24 mm for ONRTH with ka=0.115 – a limited amount of parametric roll is observed and some cases result in capsizing.

Selected results are shown and discussed in this section.

In Figure 10, the parametric roll results are presented for ONRWS (left figure) and ONRFL (right figure). For each of the hull forms, two wave slopes, ka=0.115 and 0.156 are used. Because the difference in the natural roll periods between the two ships, the incident wave length used is different for the two ships. In ONRWS runs, the wave length / ship length = 1.05 is used. As a result, the wave amplitude is 64 mm for the ka = 0.115 case and the wave amplitude is 86 mm for the ka = 0.156 case. It can be seen from the figure on the left that with larger ka (= 0.156), the range of the parametric roll for ONRWS is wider than that of smaller ka (= 0.115). It is also noticed that the maximum roll amplitude of the parametric roll is close to 50 degrees compared to less than 42 degrees for ONRTH shown in Figure 6.

Similar calculations are carried out for ONRFL with the incident wave length / ship length = 0.97, which gives a = 59 mm for ka = 0.115 and a = 43 mm for ka = 0.156. The parametric roll for ONRFL occurs at higher Froude number ranges compared to ONRWS and ONRTH (Figure 6), though the peak roll amplitude is smaller than ONRWS.

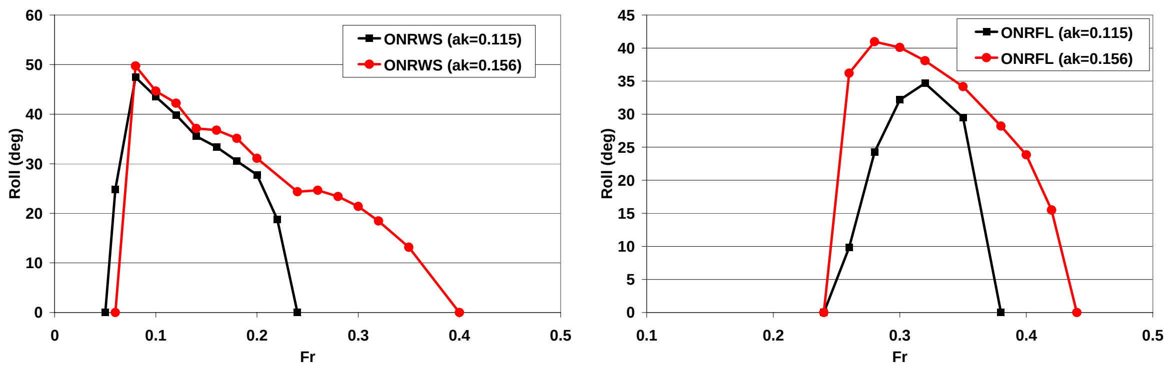

Figure 10: Roll amplitude vs. Froude number for GM=23 mm, ONRWS (left) and ONRFL

5.0 CONCLUDING REMARKS

In a previous study of post-Panamax containership, it was demonstrated that the approximate body-nonlinear hydrodynamic model of the LAMP code could qualitatively and quantitatively predict the phenomena of parametric roll in large head seas. In the present study, this approach is used to evaluate parametric roll for an unconventional surface combatant design concept incorporating a tumblehome topsides hull form.

As part of the study, LAMP predictions were compared to model tests performed for the INSEAN Ship Model 2498, which represents the tumblehome variant of the ONR Topsides hull form series. For the LAMP simulations, forward speed and GM dependent viscous roll damping models were developed based on ship model roll decay tests. Simulations were then made in regular head waves for a range of ship speeds and GM values, and limited comparison was made to the experimental results. The numerical and experiential results were qualitatively similar, but LAMP simulations showed parametric roll at a somewhat different encounter frequency range compared to the ship model test results. However, it was found that the occurrence of parametric roll in the simulation depends strongly on parameters such as roll damping, moment of inertia, GM, wave frequency, and ship speed.

To study the effects of bow flare on the parametric roll characteristics of a surface combatant, the three ONR Topside hull form variants – tumblehome (ONRTH), wall-sided (ONRWS), and flared (ONRFL) were analyzed. Based on the range of parameters studied so far, it was found that: (a) ONRWS has wider speed range within which parametric roll will occur and higher parametric roll amplitude than ONRFL and ONRTH; (b) the parametric roll tends to occur at higher Fn range for ONRFL; and (c) parametric roll is less likely for ONRTH than the other two hull forms. These results are generally consistent with the findings from the investigation of Bassler [1]. Since the difference in the parametric roll among the three ONR topsides bodies can only come from the topsides geometries (for the same GM and damping coefficients), body-nonlinearities in hydrostatic, hydrodynamic and viscous roll damping have significant effect on parametric roll.

ACKNOWLEDGEMENT

This work is funded by the Office of Naval Research. The authors would like to express their appreciation to the ONR Program Manager, L. Patrick Purtell, Ph.D., for his support of the LAMP development and this research work. We would also like to thank Prof. Fred Stern of the University of Iowa for providing INSEAN ship model 2498 model test data.

REFERENCES

[1] Bassler, C. (2008), "Application of Parametric Roll Criteria to Naval Vessels," *Proceedings of the International Ship Stability Workshop*, Seoul, Korea

[2] France, W.N., Levadon, M., Treakle, T.W., Paulling, R., Michel, R.K., and Moore, C. (2003), "An Investigation of Head-Sea Parametric Rolling and its Influence on Container Lashing Systems," Marine Technology, Vol. 10, No. 1. 2003, pp. 1-19.

[3] Hosseini, S., Park, I., Stern, F., Olivieri, A., Campana, E., and Francescutto, A., (2007), "Complementary URANS CFD and EFD for Validation Extreme Motions Predictions," *Proceedings of the 9th International Conference on Numerical Ship Hydrodynamics*, Ann Arbor, Michigan, August 5-8, 2007.

[4] Lin, W.M., and Yue, D.K.P. (1990), "Numerical Solutions for Large-Amplitude Ship Motions in the Time-Domain," *Proceedings of the Eighteenth Symposium of Naval Hydrodynamics*, The University of Michigan, U.S.A.

[5] Lin, W.M., and Yue, D.K.P. (1993), "Time-Domain Analysis for Floating Bodies in Mild-Slope Waves of Large Amplitude," *Proceedings of the Eighth International Workshop on Water Waves and Floating Bodies*, Newfoundland, Canada

[6] Lin, W.M., Zhang, S., Weems, K., and Yue, D.K.P. (1999), "A Mixed Source Formulation for Nonlinear Ship-Motion and Wave-Load Simulations," *Proceedings of the Seventh International Conference on*

Numerical Ship Hydrodynamics, Nantes, France

[7] Olivieri, A., Francescutto, A., Campana, E.F., and Stern, F. (2008), "Parametric Roll Highly Controlled Experiments for an Innovative Ship Design," OMAE Symposium, June 2008

[8] Shin, Y.S., Belenky, V.L., Paulling, J.R., Weems, K.M., and Lin, W.M., (2004), "Criteria for Parametric Roll of Large Containerships in Longitudinal Seas," SNAME Annual Meeting, 2004

[9] Weems, K., Zhang, S., Lin, W.M., Shin, Y.S, and Bennett, J. (1998), "Structural Dynamic Loadings Due to Impact and Whipping," *Proceedings of the Seventh International Symposium on Practical Design of Ships and Mobile Units*, The Hague, The Netherlands.